The Covariation of Color and Orange Fluorescence Instabilities in Yellow Sapphires

Yang, Yunqi; Wang, Chaowen; Wang, Chengsi; Shen, Xibing; Yin, Ke; Chen, Tao; Shen, Andy Hsitien; Algeo, Thomas J.; Hong, Hanlie

DOI
10.3390/min13050663

Publication date
2023

Document Version
Final published version

Published in
Minerals

Citation (APA)
Yang, Y., Wang, C., Wang, C., Shen, X., Yin, K., Chen, T., Shen, A. H., Algeo, T. J., & Hong, H. (2023). The Covariation of Color and Orange Fluorescence Instabilities in Yellow Sapphires. *Minerals*, *13*(5), Article 663. https://doi.org/10.3390/min13050663

minerals

MDPI

Article

The Covariation of Color and Orange Fluorescence Instabilities in Yellow Sapphires

Yunqi Yang [1,2], Chaowen Wang [1,2,3,*], Chengsi Wang [1,2], Xibing Shen [4,5], Ke Yin [4], Tao Chen [1,2], Andy Hsitien Shen [1,2], Thomas J. Algeo [6,7,8] and Hanlie Hong [4,7]

1 Gemmological Institute, China University of Geosciences, Wuhan 430074, China; yangyunqi@cug.edu.cn (Y.Y.); wangcs@cug.edu.cn (C.W.); summerjewelry@163.com (T.C.); shenxt@cug.edu.cn (A.H.S.)
2 Hubei Gems and Jewelry Engineering Technology Research Center, Wuhan 430074, China
3 Department of Geosciences and Engineering, Delft University of Technology, 2628 CN Delft, The Netherlands
4 School of Earth Sciences, China University of Geosciences, Wuhan 430074, China; xbshen@cug.edu.cn (X.S.); yinke@cug.edu.cn (K.Y.); honghanlie@cug.edu.cn (H.H.)
5 School of Resources and Environment, Beibu Gulf University, Qinzhou 535011, China
6 Department of Geosciences, University of Cincinnati, Cincinnati, OH 45221-0013, USA; thomas.algeo@uc.edu
7 State Key Laboratory of Biogeology and Environmental Geology, China University of Geosciences, Wuhan 430074, China
8 State Key Laboratory of Geological Processes and Mineral Resources, China University of Geosciences, Wuhan 430074, China
* Correspondence: c.w.wang@cug.edu.cn; Tel.: +86-132-9706-2002

Abstract: In recent years, some sapphires were found to fade in sunlight and to increase their color after UV irradiation. This unstable color phenomenon is attributed to the photochromism of corundum. The photochromic effect seriously affects the grading and evaluation of sapphires, although its mechanism is still uncertain. Here, we performed a set of photochromic experiments on sapphire specimens using a 254 nm shortwave UV light source and a D65 light source (which simulates sunlight) to generate different color states exhibiting characteristic absorption, emission, and excitation spectra. We observed that, for different color states, variation in the intensity of the absorption band at ~460 nm was consistent with that of orange fluorescence at 500–800 nm. This observation indicates a relationship between color instability and orange fluorescence. Peaks in excitation spectra at 320, 420, 490, 560, and 637 nm provide insight into the source(s) of excited orange fluorescence, which are related to different types of F-centers and Mg-trapped holes. We propose an explanation for the photochromic phenomenon: the color of photochromic yellow sapphire is the result of a variety of defects that release orange fluorescence simultaneously. Further, we hypothesize that the mechanism of photochromism in yellow sapphires is linked to electron transfer between F-centers and Mg-trapped holes.

Keywords: photochromic; corundum; defect; F-center; trapped hole; excitation spectrum

Citation: Yang, Y.; Wang, C.; Wang, C.; Shen, X.; Yin, K.; Chen, T.; Shen, A.H.; Algeo, T.J.; Hong, H. The Covariation of Color and Orange Fluorescence Instabilities in Yellow Sapphires. *Minerals* **2023**, *13*, 663. https://doi.org/10.3390/min13050663

Academic Editor: Thomas Hainschwang

Received: 20 March 2023
Revised: 25 April 2023
Accepted: 10 May 2023
Published: 12 May 2023

1. Introduction

Color is of great significance for the classification and evaluation of the value of a gemstone. However, in recent years, many gems with authoritative identification certificates faded or changed color to varying degrees after being displayed or worn for a period of time, which has caused serious trouble to the gemstone market. When gems are exposed to sunlight or ultraviolet light, their color changes reversibly. This color instability is called photochromism [1]. Photochromic effects are known in a variety of gemstones, including diamond [2,3], sapphire [4,5], hackmanite [6], scapolite [7], tugtupite [8], and zircon [9,10], among others. For high-value colored gemstones such as sapphire especially, subtle color changes mostly degrade the level during color classification, thus lessening their value.

Sapphire, as one of the highest-value colored gemstones exhibiting the photochromic effect, has been extensively studied. Most studies since the 1940s have focused on photographic records and descriptions of color instability [4,5,11–15]. For instance, Pough and Rogers (1947) first reported the photochromism of natural sapphire [11]. After a comprehensive study of yellow sapphire, Nassau and Valente (1987) reviewed its color origins and specifically pointed out that yellow sapphires with low iron content and colored via natural or artificial irradiation are most prone to color instability [12]. Furthermore, Williams and Williams (2016) and Zhao et al. (2018) indicated that natural, synthetic, and heat-treated yellow sapphires can display the photochromic effect, especially those from Sri Lanka and Madagascar [13,14]. Later, this phenomenon was observed not only in yellow sapphires, but also in Papalacha-like and light to colorless sapphires [5,15]. From these considerations, one may infer that the photochromic effect is related to the intrinsic characteristics of corundum crystals, which occur in a variety of colors and natural, synthetic, and heat-treated samples. The unresolved issue is the mechanism for this phenomenon.

The mechanism of photochromism is of interest not only to gemologists but also to applied scientists owing to the use of these materials in many high-tech applications in the fields of optical storage, switching components, and nuclear reactors [16–18]. Great progress has been made in uncovering the mechanism of photochromism in some types of photochromic materials. For instance, photochromic behavior in hackmanites, tugtupite, and scapolite has been explained as a product of similar S polyanionic substitutions for Cl^{-}, with the degree of color stability depending on the motion of a specific Na atom that helps to stabilize a trapped electron responsible for the coloration [1,8]. Previous studies of photochromic crystals have shown that their photochromic properties are often related to crystal lattice defects [2,3,7,8,19–21] and specifically to the movement of electrons between such defects [1].

Corundum can be used both as a gemstone (sapphire) and as an optical and catalytic material. The existence of photochromic effects and crystal lattice defects in sapphire strongly affects its optical, electrical, and thermal properties, but there is no theoretical model to explain the relationship of defects to photochromism. In previous work using three-dimensional fluorescence spectra, our group found that all sapphires exhibiting photochromic effects have a common fluorescence center emitting orange fluorescence [22]. A recent study suggested that orange fluorescence in sapphires may be related to some site vacancy defects [23]. In the present study, we carry out a photochromic experiment on Sri Lankan sapphire and compare the variation in its absorption and fluorescence spectra for different color states. The goals of this study are (1) to explain the relationship of color in sapphires to internal lattice defects, (2) to find an effective method of characterizing such defects, and (3) to formulate a physicochemical model of the photochromic behavior of sapphires exhibiting unstable colors.

2. Materials and Methods

Fourteen yellow sapphire specimens from Sri Lanka with varying color saturation, purchased from the local gem market in Ratnapura, close to the mining area, were investigated in this study. The specimens include both natural and heat-treated gemstones.

2.1. Photochromic Experiments and Fluorescence Observations

All fourteen sapphire specimens were tested for photochromism. To achieve two different color states, firstly a D65 light source was used to produce a spectrum similar to the spectrum composition of sunlight to fade the specimens, with an exposure time of 24 h. Secondly, the same specimens were colored with a shortwave ultraviolet (UV) lamp with a main wavelength of 254 nm, with an exposure time of 4 h. After being exposed to UV, the fluorescence of the 14 sapphire specimens was observed and photographed under an ultraviolet lamp with a wavelength of 365 nm.

2.2. Chemical Composition Analysis

The chemical compositions of the 14 sapphire specimens were obtained with laser ablation inductively coupled plasma mass spectrometry (LA-ICP-MS). The analysis was carried out in the State Key Laboratory of Geological Processes and Mineral Resources, China University of Geosciences-Wuhan using a GeoLas Pro laser ablation system interfaced with an Agilent 7500a ICP-MS. The test conditions were as follows: laser ablation aperture 44 μm, frequency 10 Hz, and laser energy density 6.0 mJ/cm^2. Reference materials included USGS (BCR-2G, BHVO-2G, and BIR-1G) and NIST (SRM 610) glasses as external calibration standards, and ^{27}Al was used as the normalizing element to calculate the concentrations of 55 trace elements with the ICPMS DataCal 9.0 software (State Key Laboratory of Geological Processes and Mineral Resources, China University of Geosciences-Wuhan, Wuhan, China) [24]. The values of elements are reported in units of ppma as proposed by Emmett et al. (2003), which is calculated as (1) [25]:

$$\text{ppma} = \frac{(\text{molecular weight of } Al_2O_3)/5}{(\text{atomic weight})} \bullet \text{ppmw} \quad (1)$$

where 'atomic weight' and 'ppmw' (i.e., ppm weight) refer to the element of interest. Units of parts per million atomic (ppma) are more useful for understanding elemental substitution patterns in crystals than ppmw because substitutions depend on the number of atoms rather than their masses.

We carried out chemical composition, photochromic experiments, and other basic gemological experiments on all 14 sapphire specimens [22]. On the basis of these nondestructive tests, we selected two specimens (S6 and S8) and cut them into wafers for further testing. Both S6 and S8 are natural and untreated specimens (non-heat-treated) with similar chemical compositions, but they have contrasting photochromic effects in wafers. The photochromic effect is strong for specimen S6 but weak for specimen S8.

In order to comprehensively evaluate the unstable change mode of the two wafered specimens, photochromic experiments were conducted again, and the microscopic ultraviolet-visible absorption, emission, and excitation spectra of each specimen under different color states were tested.

2.3. Micro-Ultraviolet-Visible Absorption Spectrum Test

The absorption spectroscopy of each specimen was analyzed at the Gemmological Institute, China University of Geosciences (Wuhan), using a JASCO MSC5200 micro-ultraviolet-visible-near-infrared spectrometer. The instrument is equipped with a 30 W deuterium lamp and a 20 W halogen lamp as the light sources. The spectral range is 200–1000 nm with an aperture diameter of 100 μm, a data collection interval of 0.5 nm, and a scanning speed of 1000 nm/min.

2.4. Photoluminescence Spectrum Test

We used emission spectra to explore the fluorescence characteristics of the specimens. According to the fluorescence characteristics of previous experiments [22], we selected 366, 532, and 325 nm lasers as the excitation light sources. Emission spectra were collected over the ranges of 640–800 nm, 550–800 nm, and 350–800 nm, respectively, with a recording interval of 0.1 nm. We used excitation spectra to explore the source of orange fluorescence. According to the results of the emission spectra, the emission light sources were at 560, 582, 586, 596, 619, 627, 630, 666, and 750 nm, and the corresponding excitation spectrum collection ranges were 300–540 nm, 300–562 nm, 300–566 nm, 300–576 nm, 300–599 nm, 300–607 nm, 300–646 nm, and 300–730 nm, with a recording interval of 1.0 nm. The emission spectrum of each specimen was recorded using a Horiba LabRAM HR instrument in the State Key Laboratory of Geological Processes and Mineral Resources of China University of Geosciences (Wuhan). The excitation spectrum test and the shortwave band emission spectrum test were carried out using a JASCO FP8500 photoluminescence (PL)

spectrometer equipped with a xenon lamp at the Gemmological Institute, China University of Geosciences-Wuhan.

2.5. Peak Fitting

The absorption and fluorescence spectra were peak-fitted using the Origin 2019b software. Before peak fitting, a constant background value was subtracted based on the minimum value of each spectrum. Peaks were fitted using a Gaussian distribution. Absorption spectrum fitting ranged from 300 to 800 nm, and fluorescence spectrum fitting ranged from 330 to 800 nm.

The spectroscopic experimental procedure was as follows (Figure 1):

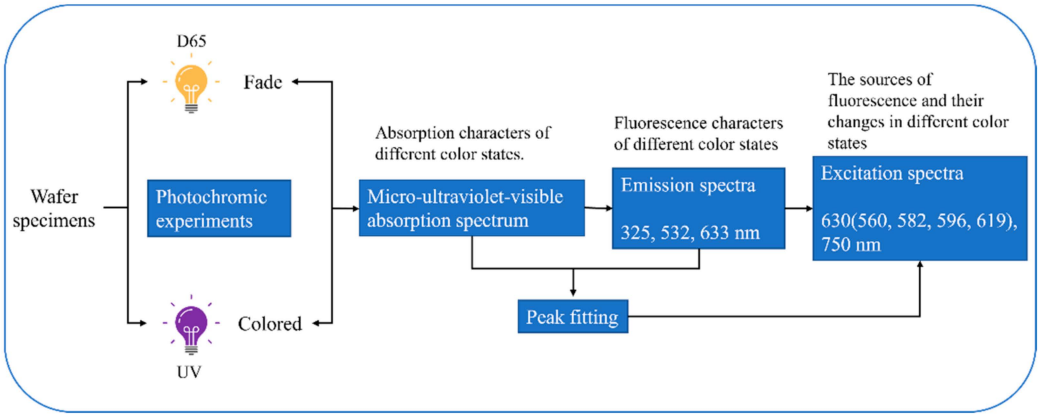

Figure 1. Flowchart illustrating experiment procedural of wafer specimens.

3. Results

3.1. Photochromic Experiments and Fluorescence Characteristics

The photochromic effect and fluorescence of all study specimens are shown in Figure 2. All fourteen sapphire specimens have different degrees of photochromic effect (including natural samples and heat-treated samples). The colors of sapphires are lightened after being exposed to D65 light and deepened after being exposed to UV light. Varying degrees of orange fluorescence were observed in all specimens, both natural and heat-treated (Figure 2). The intensity of the orange fluorescence is not dependent on the hue and saturation of the original color of each specimen. Some specimens showing high saturation have strong orange fluorescence, such as S5 and S7, whereas others have weak orange fluorescence (S6, S10, and HS1).

3.2. Chemical Composition Analyses

The results of laser ablation inductively coupled plasma mass spectrometry (LA-ICP-MS) show that, as expected for corundum, the main chemical component of the specimens is Al_2O_3. Certain trace elements are present in amounts above their detection limits, including Fe, Ti, Mg, Ga, and V (see Table 1). The Fe content ranges from 88 to 268 ppma, and that of Ga from 5 to 20 ppma. The contents of Mg, Ti, and V are 17–90, 0–19, and 1–4 ppma, respectively.

3.3. Absorption Spectra

The S6 and S8 wafer specimens, which have contrasting photochromic effects, were further tested. The absorption bands at ~330 nm and ~460 nm exhibited varying intensities between the different color states for both S6 and S8 under ultraviolet-visible spectroscopy (Figure 3a). The intensity of absorption spectra increased after UV irradiation but decreased after D65 irradiation, demonstrating that this variation is reversible. The difference between these specimens is that both absorption bands of S6 are strongly enhanced after exposure to shortwave UV light, whereas S8 exhibited enhancement only near 330 nm, which is beyond the range of visible light, but not near 460 nm. This pattern is consistent with naked-eye

observations, in which S6 showed a strong photochromic effect, whereas the color of S8 was relatively stable (Figure 3a).

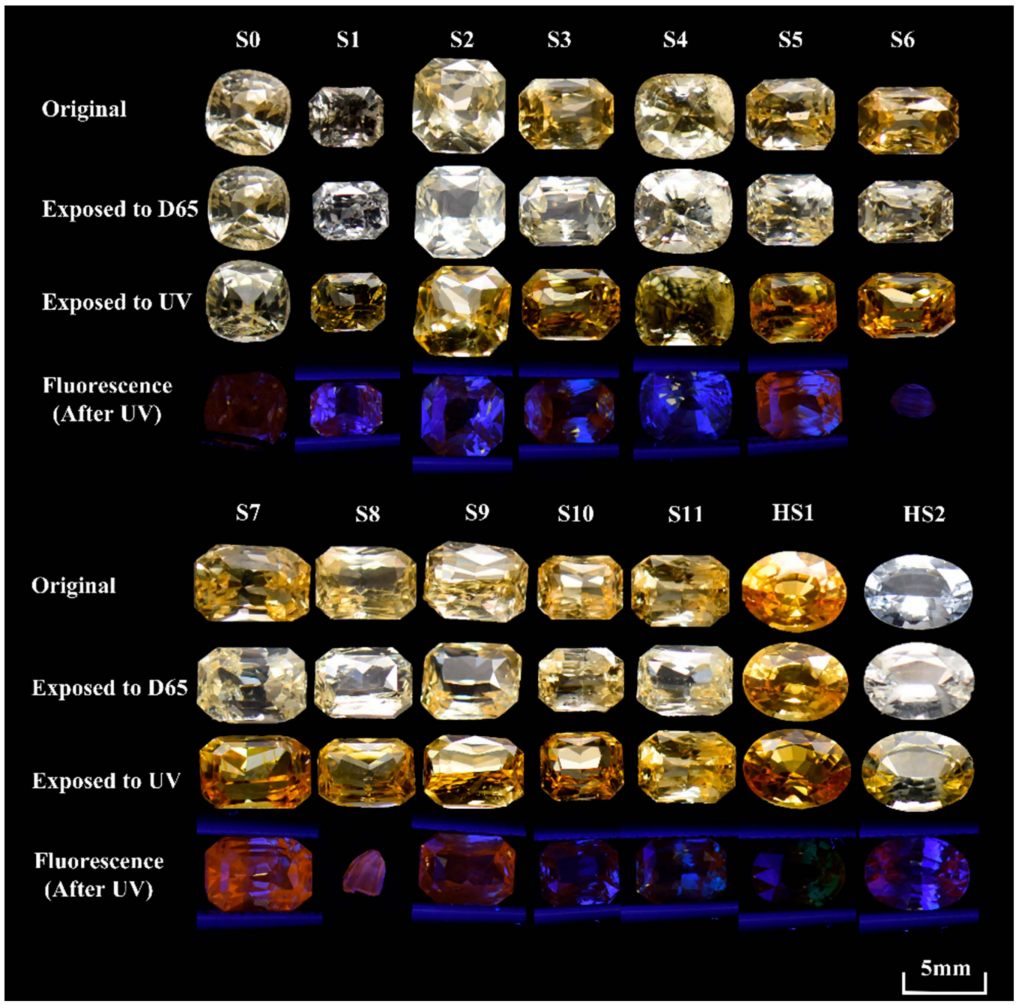

Figure 2. Photos of the study specimens and their fluorescence. Specimens labeled as S and HS are natural unheated and heated specimens, respectively. The colors of specimens are lightened after exposure to D65 light and deepened after exposure to UV light. All specimens show an orange fluorescence.

Table 1. Average concentrations of trace elements in yellow sapphire (units of ppma).

Element (ppma)	Fe	Ti	Mg	Ga	V
S1	179.1	12.68	73.38	9.40	4.30
S2	267.9	18.85	89.58	13.53	1.03
S3	97.2	9.50	35.84	9.64	1.95
S4	149.7	bdl [1]	67.68	16.62	0.60
S5	88.2	35.71	79.96	5.06	2.48
S6	136.6	20.23	38.02	11.01	1.80
S7	187.5	75.53	88.13	18.73	4.22
S8	110.6	7.94	40.97	8.12	2.63
S9	108.5	bdl	21.88	11.81	1.91
S10	157.4	8.73	16.52	18.64	0.53
S11	94.1	7.88	27.69	15.12	1.34
HS1	99.1	9.20	73.61	10.48	1.42
HS2	162.2	18.87	42.17	20.13	5.15
S0	114.4	15.71	26.30	13.65	0.55

[1] Below detection limit.

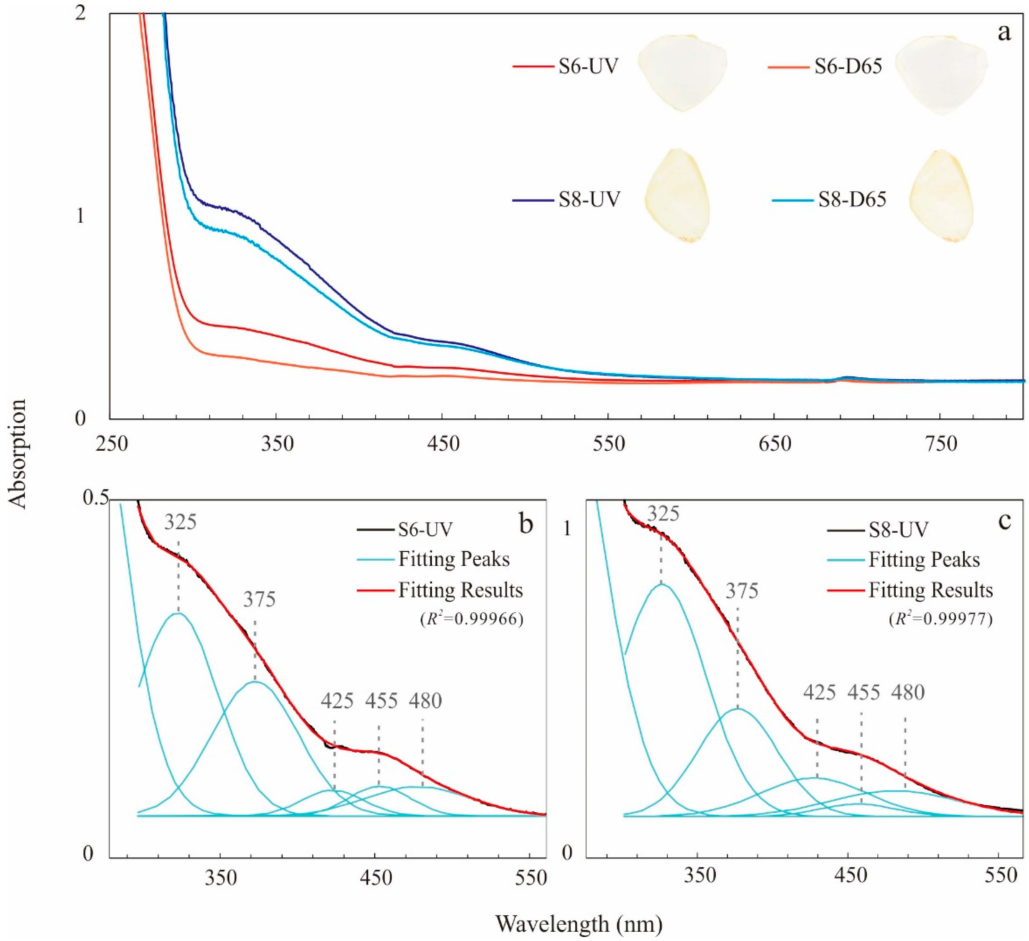

Figure 3. Absorption spectra of two natural Sri Lankan yellow sapphires exposed to UV and D65 light sources. (**a**) Absorption spectra; (**b**,**c**) Fitted absorption spectra of specimens S6 and S8 after UV irradiation, respectively.

In order to clarify the significance of the broad bands in the absorption spectrum, we fit the spectra according to the absorption characteristics of possible defects in the sapphire. The well-fitted absorption peaks are located at 325, 375, 425, 455, and 480 nm. The R^2 values of the fitting results are 0.99966 for S6 and 0.99977 for S8.

3.4. Photoluminescence Spectra

3.4.1. Emission Spectra

We used 325, 532, and 633 nm lasers as excitation light sources to obtain the emission spectra of the S6 and S8 specimens under different color states (Figures 4 and 5). In the emission spectra for the 325 nm source, both S6 and S8 are characterized by broad, strong bands from ~500 to ~800 nm in both color states, showing orange fluorescence (Figure 4a). The most intense peaks of S6 and S8 are located at 582 and 630 nm, respectively. These two fluorescence peaks are present in both S6 and S8. Specimen S8 has higher fluorescence intensity than specimen S6 (Figure 4a), which is consistent with the macroscopic observation showing that S8 has stronger fluorescence (Figure 2). For specimen S6, which exhibits a strong photochromic effect, fluorescence became stronger after D65 irradiation and weaker after UV irradiation. For specimen S8, which exhibits a relatively stable color, fluorescence intensity did not change significantly during the photochromic experiments.

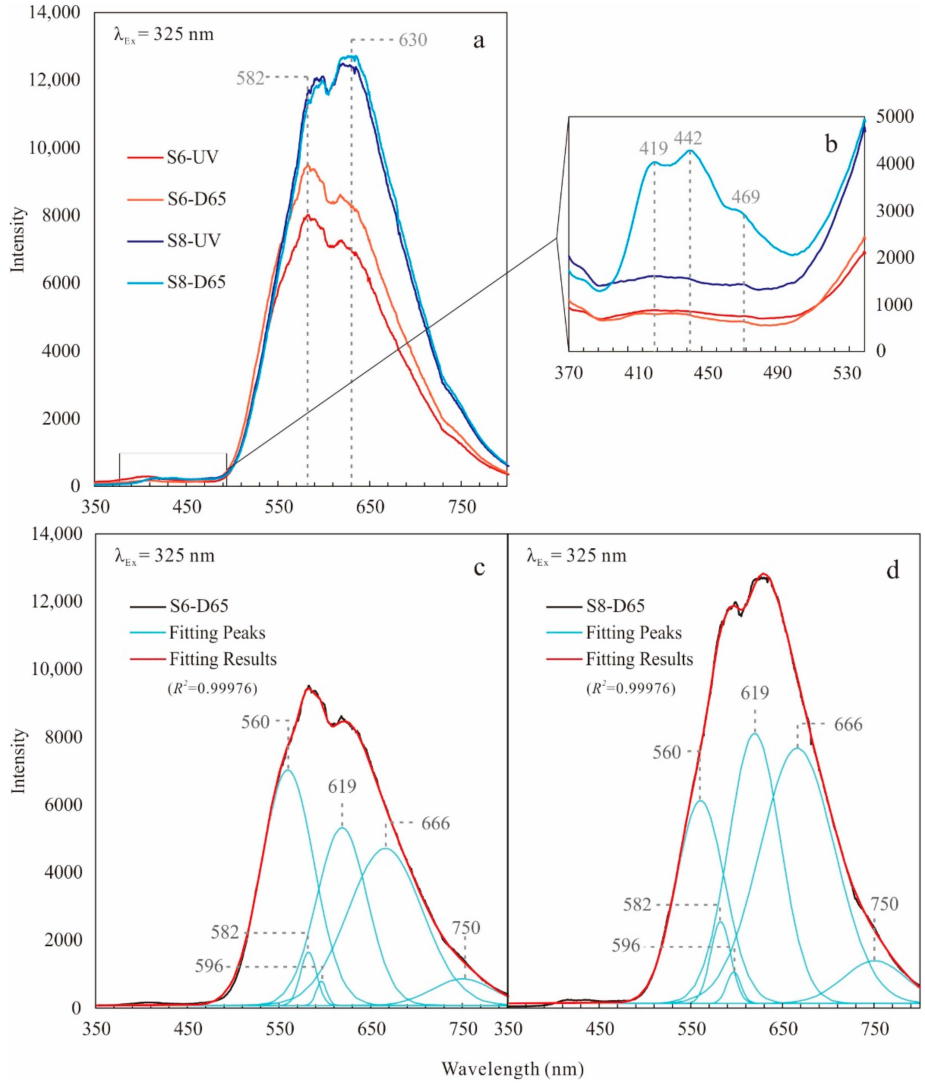

Figure 4. Emission spectra of two natural Sri Lankan yellow sapphires exposed to UV and D65 light. (**a**) Spectra generated using a Horiba LabRAM HR with a 325 nm laser source; (**b**) Spectra generated using a JASCO FP8500 fluorescence spectrometer with a xenon lamp source; (**c**,**d**) Peak fitting results of specimens S6 and S8, respectively.

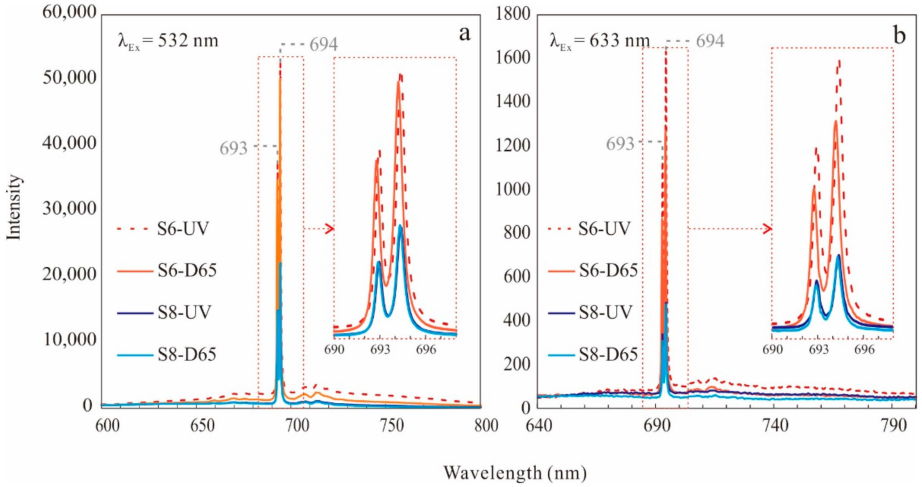

Figure 5. Emission spectra of two natural Sri Lankan yellow sapphires exposed to UV radiation. (**a**) Emission spectra using a 532 nm source; (**b**) Emission spectra using a 633 nm source.

According to the spectral pattern of this broad and strong band, possible combinations of fluorescence peaks were explored by peak fitting (Figure 4c,d). The centers of these peaks are located at 560, 582, 596, 619, 666, and 750 nm. The R^2 values of the fitting results are 0.99976 for both S6 and S8.

In order to understand the fluorescence characteristics of the shortwave part of the spectrum more clearly, we used a fluorescence photometer to recollect data for the relevant wavelengths (Figure 4b). The results show that the variation law is different from that of the longwave part of the spectrum. The fluorescence characteristics of S6 in the shortwave band are weak, and there is no change between the different color states. For S8, the fluorescence peaks of 419, 442, and 469 nm disappeared after 4 h of UV irradiation.

In the emission spectra for the 532 and 633 nm sources, we obtained similar emission features; the main fluorescence characteristics are the distinct bimodal peaks at 693 nm and 694 nm (Figure 5a,b). The emission spectrum for the 532 nm source has stronger intensity than that for the 633 nm source (Figure 5a). The emission intensity of the strong photochromic effect of S6 is slightly enhanced after UV irradiation and reduced after D65 irradiation. This change is even more pronounced for the 633 nm source (Figure 5b). For S8, which has relatively stable color, the emission intensities are almost unchanged for both the 532 and 633 nm sources.

3.4.2. Excitation Spectra

In order to explore the source of orange fluorescence in the study specimens, we tested the excitation spectra of the most intense emission (582 and 630 nm) and the characteristic peaks in the peak-fitting results (560, 582, 596, 619, 666, and 750 nm). Among them, we obtained similar results in the excitation spectra at 560, 582, 596, 619, and 630 nm (a representative spectrum at an emission wavelength of 630 nm is shown in Figure 6a). The excitation spectra of specimens S6 and S8 are composed of four peaks located at 320, 420, 490, and 561 nm. The main difference between them is in the intensity of the excitation band at 320 nm (Figure 6a). The S6 specimen, which has strong photochromic effects, exhibits a significant change of intensity between the different color states. Although the S8 specimen exhibits a stronger excitation band at 320 nm, it changed only slightly during the photochromic experiments. In the excitation spectra of 666 and 750 nm, the strongest band of fluorescence gradually shifted from 320 nm to 490–510 nm. It has four excitation peaks with weak intensities at wavelengths of 490, 510, 550, and 637 nm (Figure 6b). Specimens S6 and S8 both showed only slight changes under different color states.

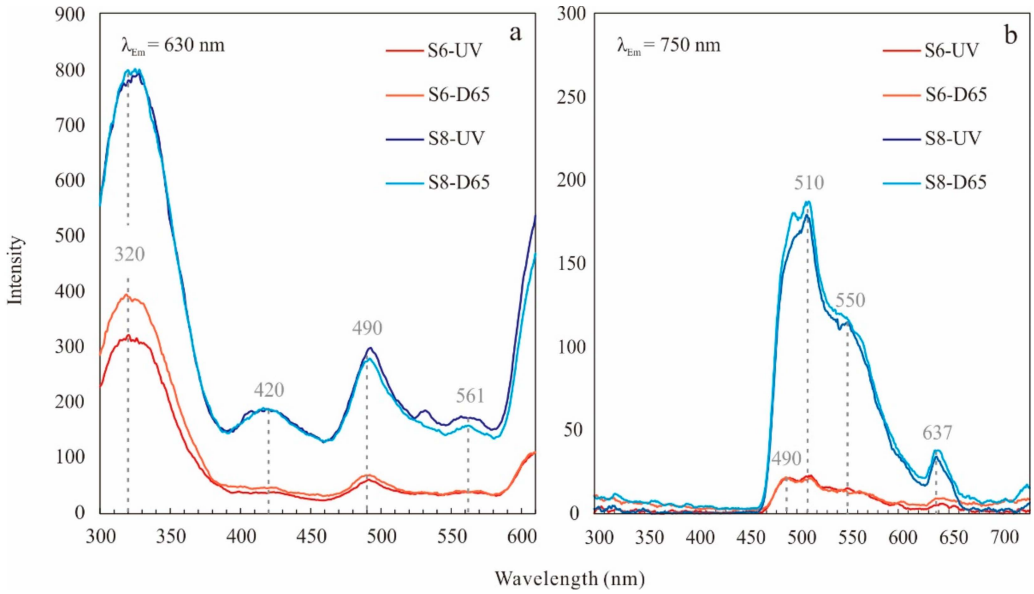

Figure 6. Excitation spectra of two natural Sri Lankan yellow sapphires exposed to UV and D65 light. (**a**) Excitation spectra using a 630 nm source; (**b**) Excitation spectra using a 750 nm source.

4. Discussion

4.1. Covariation of Color and Orange Fluorescence Instabilities

Color instability in yellow sapphires has a certain relationship to fluorescence instability, as shown by our data. A previous study showed that the 14 yellow sapphires analyzed here display different degrees of photochromic effect (including both natural and heat-treated specimens) [22]. In the macrofluorescence test, we observed that all specimens, despite their varying degrees of photochromism, showed orange fluorescence (Figure 2), which is consistent with our data obtained with a 3D fluorescence spectrometer [22]. After UV irradiation, the color of specimen S6, which exhibits a strong degree of photochromism, became deeper, the intensity of the absorption band at ~460 nm increased (Figure 3a), the orange fluorescence emission intensity at 582 and 630 nm decreased (Figure 4a), and the intensity of the strongest excitation peak of orange fluorescence at 320 nm also decreased (Figure 6a). After D65 irradiation, the color of specimen S6 became lighter, the intensity of the absorption spectrum weakened (Figure 3a), and the orange fluorescence intensity increased (Figures 4a and 6a). In contrast, specimen S8, which has a relatively stable color, showed almost no change in color and intensity of orange fluorescence after both UV and D65 irradiation. On this basis, it is possible to connect changes in the fluorescence spectrum to changes in the absorption spectrum (Figure 7). We infer that the larger the color change in a specimen, the larger the change in orange fluorescence intensity. For specimens with strong photochromism, the orange fluorescence instability is also strong.

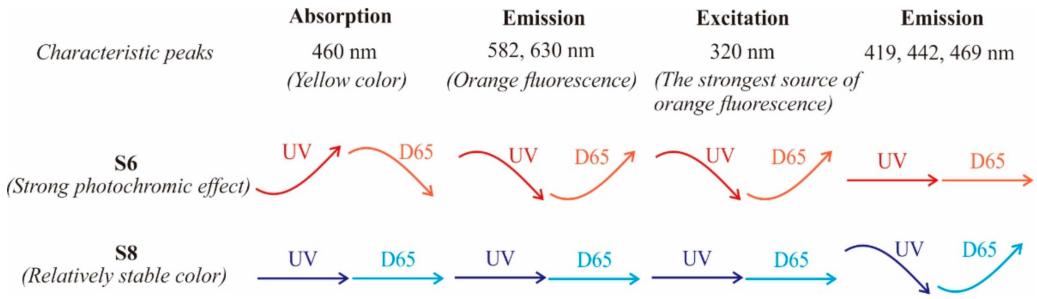

Figure 7. Characteristics of absorption, emission, and excitation spectra. Upward and downward arrows represent increases and decreases in intensity, respectively. Note that, for specimens with a strong photochromic effect, orange fluorescence intensity is also unstable.

4.2. Potential Mechanism of Photochromism in Yellow Sapphires

The yellow color in the study specimens is mainly derived from Mg-related defects (trapped holes and F-centers) that are not caused by iron. There are two main sources of yellow in corundum, reflecting traditional causes of color. One is related to Fe^{3+}, which can exist as single ions replacing Al^{3+}, Fe^{3+}-Fe^{3+} pairs, and possibly larger Fe^{3+} clusters, but with less chromatic ability, producing a weak lemon-yellow color only when the Fe^{3+} concentration is greater than 2500 ppma [26,27]. The other is related to Mg-trapped holes. When Mg^{2+} substitutes isomorphically for Al^{3+} in the crystal lattice, the charge deficiency is typically compensated by tetravalent impurities (such as Si and Ti) [25,28,29], but when tetravalent ions are in insufficient supply, it is compensated by an oxygen vacancy or a hole. When Mg^{2+} is charge-compensated by a hole, it behaves as an O^- (i.e., an oxygen ion carrying a charge of −1 rather than −2) in the lattice [25] (Figure 8a). Mg^{2+}-induced trapped holes ($h^\bullet$) often combine with other contaminant ions to produce color [30]. When Mg^{2+} is charge-compensated by oxygen vacancies, F-center defects often appear (Figure 8b). The F-center is a crystal defect in which an anionic vacancy in a lattice is occupied by one or more unpaired electrons. Irradiation, crystal growth, and artificial irradiation treatment may produce such defects. According to the number of electrons, an F-center is often divided into F (where a single oxygen vacancy is occupied by two electrons), F^+ (where a single oxygen vacancy is occupied by one electron), and their aggregates F_2 (where four electrons are captured), F_2^+ (where three electrons are captured), and F_2^{2+} (where two electrons are

captured). F-centers also cause absorption in the UV-VIS wavelengths [31–35]. Although they are intrinsic defects, the formation of an F-center in sapphire is often associated with Mg. Mg-doped Al_2O_3 crystals are more likely to produce oxygen vacancies and higher-order defects than undoped ones [36]. In both S6 and S8, the Fe content was very low, far less than 2500 ppma (Table 1), and the characteristic peaks related to Fe^{3+} were not observed in their absorption spectra. It can be inferred that the yellow color in the study specimens was not caused by substitution of Al^{3+} with Fe^{3+}, and it may have been caused mainly by Mg^{2+}-trapped holes and other related defects. This is consistent with previous observations of the chemical composition of photochromic yellow sapphires [12].

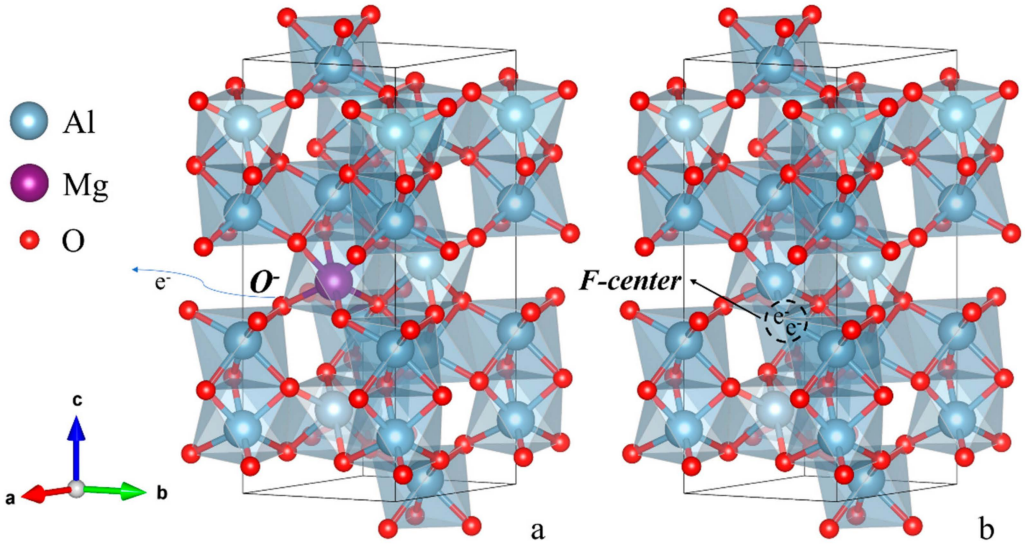

Figure 8. Defects in the sapphire crystal lattice. (**a**) Mg-trapped holes bonded with O^-; (**b**) F-center.

The yellow color produced by photochromism is related to defects in producing orange fluorescence. Previous research has shown that yellow sapphires with unstable color often have low iron content and are colored by Mg-trapped holes [12,14]. However, not all yellow sapphires that are colored by Mg-trapped holes fade to colorlessness after exposure to sunlight [12]. This shows that Mg-trapped holes are not the only factor controlling color stability or causing photochromism. In our experiment, we found that the color instability of yellow sapphire was linked to fluorescence instability (Figure 7), which indicates that the defects producing orange fluorescence are probably related to its photochromic properties.

Although various theories regarding photochromism in crystals have been proposed, they generally follow classical electronic theory at the atomic level. Specifically, lattice defects create an electronic level in the band gap, absorbing visible light and producing color. The energy level of the defect controls its ability to trap electrons. Electrons are trapped when exposed to relatively high energy, such as ultraviolet light. This creates a color center, which changes the absorption spectrum and the color of the specimen. After the captured electrons absorb low-energy visible light, the crystal is brought back to its original condition through conduction of the electrons away from the defect, so that its color is restored [1].

Based on the above general principle of photochromism, and compared with our previous studies, the vacancy defect was taken into account in the attribution of spectral peaks. In their absorption spectra, the S6 and S8 specimens have two wide bands near 330 nm and 460 nm, which are likely to be a composite of absorption peaks of various elements after peak fitting (Figure 3), including F_2^+ (357 nm), F_2^+ (2·Mg) (F_2^+ bound to 2·Mg, 325 nm), F_2^{2+} (450 nm), F_2^{2+} (2·Mg) (F_2^{2+} bound to 2·Mg, 435 nm), h· (480 nm), and other defects [32,34,35]. In the fluorescence spectra, we also found features related to these defects. Orange fluorescence is mainly excited by 320, 420, 490, 561, and 637 nm wavelengths, which correspond to F^+, F_2^{2+} (2·Mg), divalent ion-related holes, F_2^{2+}, and

F_2^+ (2·Mg), respectively [23,32–35,37–39]. The F^+-center at 320 nm contributes the most orange fluorescence, and it changes most strongly during the process of photochromism (Figure 6a). Therefore, we infer that, among the above defects contributing to orange fluorescence in sapphires, the change of F^+-center likely dominates the instability of orange fluorescence linked to photochromism.

We also found that specimen S8, which has a relatively stable color, shows varying characteristics in the shortwave band of the emission spectrum. The three main fluorescence peaks in the shortwave band of its emission spectrum are at 419, 442, and 469 nm, which have been linked to F-, 'F-type'-, and F_2^{2+}-(type II)-centers, respectively [23,31,32,40]. During the photochromic experiment, these three fluorescence peaks showed significant changes. However, specimen S6, which has an unstable color, does not show similar changes (Figure 5b). For this reason, we infer that the defects associated with the fluorescence peaks at 419, 442, and 469 nm are indispensable for color stability (Figure 7).

Based on the inferred relationship between lattice defect concentrations and the process of photochromism, we offer the following conjecture about internal changes in the crystal lattice. In specimen S6, irradiation with D65 caused electrons to escape from oxygen vacancies, increasing F^+-center concentrations. The escaped electrons entered the Mg-trapped holes and filled them, making the specimen lighter in color. However, after UV irradiation, the electron charging process reversed, leading to a decrease in F^+-center concentrations, an increase in trapped-hole concentrations, and a deepening of specimen color. These changes can be represented by the following model reactions:

$$V_o \overset{h\vartheta_1}{\rightarrow} F^+ + e^-, \text{ then } O^- + h^\bullet + e^- \rightarrow O^{2-}$$

$$O^{2-} \overset{h\vartheta_2}{\rightarrow} O^- + h^\bullet + e^-, \text{ then } F^+ + e^- \rightarrow V_o$$

where $h\vartheta_1$ = visible light, and $h\vartheta_2$ = 254 nm.

In specimen S8, D65 irradiation preferentially excited the defects associated with fluorescence peaks at 419 nm, 442 nm, and 469 nm. F^+-center concentrations, trapped-hole concentrations, and specimen color all remained unchanged. After UV irradiation, the defects associated with these fluorescence peaks were preferentially eliminated, causing F^+-center concentrations, trapped-hole concentrations, and specimen color to remain unchanged.

4.3. Implications and Limitations of the Photochromic Mechanism in Yellow Sapphires

We encountered some difficulties in this study that warrant explanation. The first is the role of Cr^{3+} in the photochromic mechanism. Cr^{3+} combined with Mg^{2+}-induced trapped holes ($h^\bullet$) was considered to produce color in previous studies [30]. Cr^{3+} accounts for the fluorescence characteristics of the 693 and 694 nm peaks [41] in the emission spectra for 532 and 633 nm as excitation sources (Figure 5a,b), even though Cr^{3+} cannot be detected by ICP-MS analysis because of its low concentration in the study specimens. We observed that the fluorescence instability of Cr^{3+} is related to the color instability of specimens (Figure 5), and we suspect that the positive correlation between Cr fluorescence and absorption intensity change is a chain effect in the photochromic process, but we have not found direct evidence for this mechanism.

A second difficulty is the assignment of spectral peaks. Although earlier studies have investigated F-centers in sapphires, the attribution of spectral peaks is still problematic due to the complexity of crystal defects. Differences in the environment around an F-center can cause changes in the peak positions of its optical absorption spectrum [33]. For example, compared with a simple F_2^{2+}-center, the absorption band and fluorescence band of the F_2^{2+}-(2·Mg)-center, in which two Mg ions are connected, exhibit significant blue shifts (435 nm vs. 459 nm and 520 nm vs. 563 nm, respectively) [33]. In addition, complex defects such as the 'F-type' remain poorly documented [40], and we still do not understand its structure and conversion mechanism.

Furthermore, not yet fully understood are interconversions among different types of F-centers when subjected to external energy. For example, in crystals containing a large number of F_2^{2+} defects, photoexcited electrons of 5.0 eV are captured by the F_2^{2+}- and F_2^{+}-centers, thus converting the F_2^{2+}-centers to F_2^{+}-centers [36]. Moreover, the conversion occurs not only between defect aggregates (F_2-type), but also between monomers and aggregates (F-type and F_2-type). Irradiation with 303 nm light causes F_2-center ionization and converts them to F_2^{+}-centers, whereas the photoexcited electrons generated in the conduction band are captured by F^{+}-centers, converting them to F-centers. Irradiation with 225 nm light causes the opposite process, that is, after an F-center is ionized, an F_2^{+}-center captures the photoexcited electrons to form an F_2-center [42]. Such complex defect transformations make it more difficult to understand internal changes in the sapphire lattice during the photochromic process. To solve these problems, in the next step of our research, we will increase the number of specimens analyzed and conduct additional tests, such as electron paramagnetic resonance (EPR) analysis, in order to gain a more detailed understanding of the changes inside the crystal during the photochromic process. At the same time, the relationship between photochromism and irradiation wavelength, irradiation time, and irradiation intensity will be determined by meta-analysis of a large dataset.

Many testing institutions have added the fading test to yellow sapphire, but it is difficult to avoid the problem that the color cannot be completely restored before and after the test. If the specific changes of defects in the photochromic process can be clearly understood, the fluorescence test is expected to become a new, non-destructive, and effective detection method.

5. Conclusions

In this study, the photochromic effect of sapphires with low iron content and distinct color centers was studied via photochromic experiments. By establishing the relationship between absorption spectra and fluorescence spectra, we found that the color instability of yellow sapphires shows a certain dependence on fluorescence instability during photochromism. A new explanation for the color of photochromic yellow sapphire is proposed, attributing it to a combination of lattice defects. We infer that the defect that releases orange fluorescence plays a crucial role in the photochromic effect of yellow sapphires, which is linked to electron transfer between defects during the photochromic process. These findings indicate that fluorescence spectroscopy can be used as a means to identify color center defects in sapphires, and that the study of orange fluorescence in yellow sapphires may be an effective way to explore the relationship of lattice changes to color instability.

Author Contributions: Y.Y. and C.W. (Chaowen Wang) designed the experiments, wrote the initial manuscript, and drew all the figures in this manuscript. Y.Y. carried out the analyses. C.W. (Chengsi Wang), X.S., K.Y., T.C., A.H.S., T.J.A. and H.H. provided substantial comments and editorial revisions to the manuscript. All authors have read and agreed to the published version of the manuscript.

Funding: This research was funded by the National Science Foundation of China (grant number 42072056). Chaowen Wang acknowledges the grant from the Chinese Scholarship Council (CSC) to support him as a visiting scholar in TU Delft. Thanks for grants from Hubei Gems and Jewelry Engineering Technology Research Center (grant number CIGTXM-04-S202102).

Data Availability Statement: The authors confirm that the data supporting the findings of this study are available within the article.

Acknowledgments: The authors would like to thank Yuyan Wang for the analysis of LA-ICP-MS and photographing of specimens. Great thanks for patient help and advice to Jia Liu and Tian Shao.

Conflicts of Interest: The authors declare no conflict of interest.

References

1. Blumentritt, F.; Fritsch, E. Photochromism and Photochromic Gems: A Review and Some New Data (Part 1). *J. Gemmol.* **2021**, *8*, 780–800. [CrossRef]
2. Byrne, K.S.; Chapman, J.G.; Luiten, A.N. Photochromic charge transfer processes in natural pink and brown diamonds. *J. Phys. Condens. Matter* **2014**, *26*, 35501. [CrossRef]
3. Fritsch, E.; Delaunay, A. What Truly Characterises a Chameleon Diamond? An Example of an Atypical 25.85 ct Stone. *J. Gemmol.* **2018**, *36*, 142–151.
4. Schiffman, C.A. Unstable colour in a yellow sapphire from Sri Lanka. *J. Gemmol.* **1981**, *17*, 615–618. [CrossRef]
5. Krzemnicki, M.S.; Klumb, A.; Braun, J. Unstable colouration of Padparadscha-like sapphires. *J. Gemmol.* **2018**, *36*, 346–354. [CrossRef]
6. Kondo, D.; Beaton, D. Hackmanite/Sodalite from Myanmar and Afghanistan. *Gems Gemol.* **2009**, *45*, 38–43. [CrossRef]
7. Blumentritt, F.; Latouche, C.; Morizet, Y.; Caldes, M.T.; Fritsch, E. Unravelling the Origin of the Yellow-Orange Luminescence in Natural and Synthetic Scapolites. *J. Phys. Chem. Lett.* **2020**, *11*, 4591–4596. [CrossRef]
8. Colinet, P.; Byron, H.; Vuori, S.; Lehtiö, J.; Laukkanen, P.; Van Goethem, L.; Lastusaari, M.; Le Bahers, T. The structural origin of the efficient photochromism in natural minerals. *Proc. Natl. Acad. Sci. USA* **2022**, *119*, e2202487119. [CrossRef]
9. Suthiyuth, R. Tenebrescent Zircon. *Gems Gemol.* **2014**, *50*, 156–157.
10. Lin, S.; Chou, Y.; Huang, K. A Zircon with Strong Photochromic Effect. *Gems Gemol.* **2022**, *58*, 252–254.
11. Pough, F.H.; Rogers, T.H. Experiments in X-ray irradiation of gem stones. *Am. Mineral.* **1947**, *32*, 31–43.
12. Nassau, K.; Valente, G.K. The Seven Types of Yellow Sapphire and their Stability to Light. *Gems Gemol.* **1987**, *23*, 222–231. [CrossRef]
13. Williams, C.; Williams, B. Yellow sapphire with unstable colour-in reverse. *J. Gemmol.* **2016**, *35*, 18–19.
14. Zhao, B.; Zhi, Y.; Lyu, X.; Wang, Y. Tenebrescence of Sapphire. *J. Gems Gemmol.* **2018**, *20*, 1–14.
15. Smith, C.P.; Chaipaksa, M.; Perlmutter, A.; Vasquez, L.; Zellagui, R.; Chen, S. Heated Sapphires with Unstable Colour Centres. *J. Gemmol.* **2019**, *36*, 602–604. [CrossRef]
16. Sasajima, N.; Matsui, T.; Furuno, S.; Hojou, K. Damage accumulation in Al_2O_3 during H_2^+ or He^+ ion irradiation. *Nucl. Instrum. Methods Phys. Res.* **1999**, *148*, 745–751. [CrossRef]
17. Irie, M.; Fukaminato, T.; Matsuda, K.; Kobatake, S. Photochromism of Diarylethene Molecules and Crystals: Memories, Switches, and Actuators. *Chem. Rev.* **2014**, *114*, 12174–12277. [CrossRef]
18. Park, J.; Feng, D.; Yuan, S.; Zhou, H.C. Frontispiece: Photochromic Metal-Organic Frameworks: Reversible Control of Singlet Oxygen Generation. *Angew. Chem. Int. Ed.* **2015**, *54*, 430–435. [CrossRef] [PubMed]
19. Norrbo, I.; Curutchet, A.; Kuusisto, A.; Mäkelä, J.; Laukkanen, P.; Paturi, P.; Laihinen, T.; Sinkkonen, J.; Wetterskog, E.; Mamedov, F.; et al. Solar UV index and UV dose determination with photochromic hackmanites: From the assessment of the fundamental properties to the device. *Mater. Horiz.* **2018**, *5*, 569–576. [CrossRef]
20. Badour, Y.; Jubera, V.; Andron, I.; Frayret, C.; Gaudon, M. Photochromism in inorganic crystallised compounds. *Opt. Mater. X* **2021**, *12*, 100110. [CrossRef]
21. Vuori, S.; Colinet, P.; Lehtiö, J.; Lemiere, A.; Norrbo, I.; Granström, M.; Konu, J.; Ågren, G.; Laukkanen, P.; Petit, L.; et al. Reusable radiochromic hackmanite with gamma exposure memory. *Mater. Horiz.* **2022**, *9*, 2773–2784. [CrossRef] [PubMed]
22. Wang, Y.; Yang, L.; Li, M.; Yang, P.; Shen, A.H.; Wang, C. Spectral Characteristics and Color Origin of Unstable Yellow Sapphire. *Spectrosc. Spect. Anal.* **2021**, *41*, 2611–2617.
23. Vigier, M.; Fritsch, E.; Segura, O. Orange luminescence of corundum an atypical origin for gemmologists. *Rev. Gemmol. AFG* **2021**, *211*, 12–19.
24. Liu, Y.; Hu, Z.; Gao, S.; Günther, D.; Xu, J.; Gao, C.; Chen, H. In situ analysis of major and trace elements of anhydrous minerals by LA-ICP-MS without applying an internal standard. *Chem. Geol.* **2008**, *257*, 34–43. [CrossRef]
25. Emmett, J.L.; Scarratt, K.; Mcclure, S.F.; Moses, T.; Kane, R.E. Beryllium Diffusion of Ruby and Sapphire. *Gems Gemol.* **2003**, *39*, 84–135. [CrossRef]
26. Mcclure, D.S. Optical spectra of transition-metal ions in corundum. *J. Chem. Phys.* **1962**, *36*, 2757–2779. [CrossRef]
27. Eigenmann, K.; Kurtz, K.; Günthard, H.H. The optical spectrum of α-Al_2O_3:Fe_3^+. *Chem. Phys. Lett.* **1972**, *13*, 54–57. [CrossRef]
28. Mohapatra, S.K.; Kröger, F.A. Defect Structure of α-Al_2O_3 Doph with Magnesium. *J. Am. Ceram Soc.* **1977**, *60*, 141–148. [CrossRef]
29. Wang, H.A.; Lee, C.H.; Kr Ger, F.A.; Cox, R.T. Point defects in α-Al_2O_3:Mg studied by electrical conductivity, optical absorption, and ESR. *Phys. Rev. B* **1983**, *27*, 3821–3841. [CrossRef]
30. Dubinsky, E.V.; Stone-Sundberg, J.; Emmett, J.L. A Quantitative Description of the Causes of Color in Corundum. *Gems Gemol.* **2020**, *56*, 2–28. [CrossRef]
31. Pogatshnik, G.J.; Chen, Y.; Evans, B.D. A Model of Lattice Defects in Sapphire. *IEEE Trans. Nucl. Sci.* **1987**, *34*, 1709–1712. [CrossRef]
32. Evans, B.D.; Pogatshnik, G.J.; Chen, Y. Optical properties of lattice defects in α-Al_2O_3. *Nucl. Instrum. Methods Phys. Res.* **1994**, *91*, 258–262. [CrossRef]
33. Akselrod, M.S.; Akselrod, A.E.; Orlov, S.S.; Sanyal, S.; Underwood, T.H. Fluorescent Aluminum Oxide Crystals for Volumetric Optical Data Storage and Imaging Applications. *J. Fluoresc.* **2003**, *13*, 503–511. [CrossRef]

34. Sanyal, S.; Akselrod, M.S. Anisotropy of optical absorption and fluorescence in Al_2O_3:C,Mg crystals. *J. Appl. Phys.* **2005**, *98*, 33518. [CrossRef]
35. Sykora, G.J.; Akselrod, M.S. Photoluminescence study of photochromically and radiochromically transformed Al_2O_3:C,Mg crystals used for fluorescent nuclear track detectors. *Radiat. Meas.* **2010**, *45*, 631–634. [CrossRef]
36. Ramírez, R.; Tardío, M.; González, R.; Santiuste, J.E.M.; Kokta, M.R. Optical properties of vacancies in thermochemically reduced Mg-doped sapphire single crystals. *J. Appl. Phys.* **2007**, *101*, 123520. [CrossRef]
37. Kulis, P.A.; Springis, M.J.; Tale, I.A.; Vainer, V.S.; Valbis, J.A. Impurity-Associated Colour Centres in Mg- and Ca-Doped Al_2O_3 Single Crystals. *Phys. Status Solidi B* **1981**, *104*, 719–725. [CrossRef]
38. Atobe, K.; Nishimoto, N.; Nakagawa, M. Irradiation-Induced Aggregate Centers in Single Crystal Al_2O_3. *Phys. Status Solidi A* **1985**, *89*, 155–162. [CrossRef]
39. Fritsch, E.; Chalain, J.P.; Hnni, H.; Devouard, B.; Maitrallet, P. Le nouveau traitement produisant des couleurs orange à jaune dans les saphirs. *Rev. Gemmol.* **2003**, *147*, 11–23.
40. Ananchenko, D.V.; Nikiforov, S.V.; Kuzovkov, V.N.; Popov, A.I.; Ramazanova, G.R.; Batalov, R.I.; Bayazitov, R.M.; Novikov, H.A. Radiation-induced defects in sapphire single crystals irradiated by a pulsed ion beam. *Nucl. Instrum. Methods Phys. Res. Sect. B Beam Interact. Mater. At.* **2020**, *466*, 1–7. [CrossRef]
41. Dodd, D.M.; Wood, D.L.; Barns, R.L. Spectrophotometric Determination of Chromium Concentration in Ruby. *J. Appl. Phys.* **1964**, *35*, 1183–1186. [CrossRef]
42. Itou, M.; Fujiwara, A.; Uchino, T. Reversible Photoinduced Interconversion of Color Centers in α-Al_2O_3 Prepared under Vacuum. *J. Phys. Chem. C* **2009**, *113*, 20949–20957. [CrossRef]